buildings

MDPI

Article

Influence of Natural Fiber Derived from Agricultural Waste on Durability and Micro-Morphological Analysis of High-Strength Concrete

A. Rajkohila *, S. Prakash Chandar and P. T. Ravichandran

Department of Civil Engineering, SRM Institute of Science and Technology, Kattankulathur 603203, India
* Correspondence: ra8652@srmist.edu.in; Tel.: +91-959-766-1283

Abstract: This research focuses on the investigation of durability behavior and microstructural analysis for M70 grade of high-strength concrete (HSC) with the influence of alccofine, banana fiber (BF), and coir fiber (CF). In this investigation, cement was partly supplanted by 15% of alccofine content in weight. Two types of natural fibers, banana and coir fibers, were selected and added in concrete at 0.5%, 1%, 1.5%, and 2% by volume. Durability characteristics, such as long-term compressive performance, rapid chloride penetration, sorptivity, water absorption, volume of permeable voids, and acid attack resistance are investigated elaborately and correlate with conventional HSC. Results showed that the incorporation of banana and coir fibers with alccofine in HSC exhibited good durability performance as correlated with conventional HSC. At 180 days of curing, incorporating 1% of banana fiber increased the durability performance compared to reference HSC. Nonetheless, the high-fiber percentage of HSC has a slight reduction in durability characteristics. Among the two types of fibers, the banana fiber showed the most significant improvement in the durability properties of HSC. The influence of natural fiber on the microstructural characteristics of HSC was evaluated using scanning electron microscope (SEM), X-ray diffraction (XRD), and Fourier transform infrared (FTIR) to substantiate the experimental findings. In contrast, using additional supplementary cementitious materials (SCMs) in HSC fabrication significantly reduces cement usage and carbon emissions.

Keywords: alccofine; banana fiber; coir fiber; durability behavior; HSC; microstructural analysis

check for updates

Citation: Rajkohila, A.; Prakash Chandar, S.; Ravichandran, P.T. Influence of Natural Fiber Derived from Agricultural Waste on Durability and Micro-Morphological Analysis of High-Strength Concrete. *Buildings* **2023**, *13*, 1667. https://doi.org/10.3390/buildings13071667

Academic Editor: Andreas Lampropoulos

Received: 29 May 2023
Revised: 24 June 2023
Accepted: 27 June 2023
Published: 29 June 2023

Copyright: © 2023 by the authors. Licensee MDPI, Basel, Switzerland. This article is an open access article distributed under the terms and conditions of the Creative Commons Attribution (CC BY) license (https://creativecommons.org/licenses/by/4.0/).

1. Introduction

Concrete is the most widely used composite material in the construction sector owing to its superior compressive strength, the versatility of structural engineering applications, and durability [1]. Concrete behaves weakly under tension but firmly under compression [2]. Furthermore, it exhibits a brittle behavior and does not permit transfer stresses after cracks [3–5]. The advancement of materials technology and research has proved that fibers can also be used in concrete production, especially in high-strength concrete (HSC) to promote structural integrity, avoid brittle failure, and provide ductility for the structure [6–9]. ACI standard [10] classifies fiber into steel, glass, synthetic, and natural. Using synthetic fiber reinforcements is an expensive and non-green environment for the construction sector. In accordance with several studies, fibers could also improve the mechanical properties of concrete. Ismail Shah et al. [11] compared the static properties of coir fiber-reinforced concrete (CFRC), sisal fiber-reinforced concrete (SFRC), and hybrid fiber-reinforced concrete (HFRC) and concluded that HFRC had a 0.5% concentration increase in compressive strength over CFRC and SFRC. According to research by Wanpeng Long et al. [7], Masson pine needle fiber (MPNF) can improve the flexibility and toughness of concrete and its compressive, splitting, and rupture moduli. Thamer Alomayri et al. [12] showed that adding 0.25% of coconut fiber with ground blast furnace slag (GBFS) in recycled aggregate concrete enhanced the mechanical and durability performance.

To create HSC with higher tensile strength, the use of agricultural waste fibers may be a feasible alternative [12]. Among the different types of fibers, natural fiber is employed in concrete production owing to its numerous applications due to its vastness, quick accessibility, and green credential nature. Natural fibers comprise cellulose, hemicellulose, lignin, pectin, and wax [13–15]. The usage of cellulosic fibers, such as abaca, banana, coir, pineapple, jute, sisal, henequen, flax, hemp, etc., has been examined in several researches [16–18]. In the current scenario, research on agricultural waste has become a hotspot in civil engineering. In manufacturing concrete, natural fiber was used as an effective way to deal with agricultural waste, which could promote environmental protection while also achieving good tensile strength efficiency [19,20]. One of the significant fruit crops grown in tropical regions is the banana. The biomass produced by banana farming is enormous and wasted, but the above-ground portions, such as the pseudostem and peduncle, are significant sources of fiber. The construction sector can use banana fiber as a raw material to make concrete. Another significant agricultural crop is the coconut, wherein after the coconut fruit is harvested, the outer layer of the coconut husk is discarded. The waste coconut husk is processed to create coir fiber. However, coir fiber can be utilized to develop a range of goods, such as furniture, carpets, and brooms. It can be used as a fiber reinforcement for concrete, increasing the structure's strength and durability [21]. In many construction projects today, attention is increasingly paid to natural fiber as a potential reinforcing material [14]. Nonetheless, in the implementation of reinforced concrete structures, the use of banana and coir fibers is still in its infancy, and further research is necessary [22,23]. The feasibility of utilizing these naturally occurring and sustainable resources for construction leads to the development of eco-friendly materials and innovations in engineering technology [24].

On the other hand, strength and durability are essential components of HSC [25,26]. However, given the lifespan of a structure, the durability of concrete has emerged as a crucial subject of research interest [27]. Supplementary cementitious materials (SCMs) are pozzolanic materials which are used to increase the strength and durability of concrete. SCMs lower the amount of CO_2 emitted into the atmosphere due to the manufacture of cement. The most frequently used SCMs in the manufacture of concrete are fly ash and silica fume metakaolin. Alccofine, a by-product of blast furnace slag, is one of the supplementary cementitious materials composed of SiO_2, CaO, Fe_2O_3, and MgO, and can be used to increase the durability aspects of HSC.

This study aims to fill a gap in existing research by investigating the combined effects of banana fiber, coir fiber, and alccofine on HSC's mechanical and durability characteristics. While previous studies have examined the individual effects of these materials, more research needs to be carried out on their combined influence. Understanding the synergistic effects can significantly enhance the durability properties of concrete. Therefore, this study examines the impact of alccofine with various proportions of banana and coir fibers on the durability of concrete as well as its microstructural behavior at different curing ages.

2. Experimental Program

2.1. Materials

Ordinary Portland cement (OPC) of grade 53, in accordance with IS 12269: 2013 [28], was utilized as a binder for all combinations. The oxide composition of the binder material is displayed in Table 1. The cement characteristics were identified in accordance with IS 4031 (Part 4): 1988 [29] and IS 4031 (Part 5): 1988 [30], as shown in Table 2. Moreover, in accordance with IS 383: 2016 [31] grading, zone III-compliant fine aggregate was passed through a 4.75 mm sieve and coarse aggregates were retained on a 10 mm screen after passing through a 12.5 mm sieve that was selected for making concrete. The specific gravity, bulk density, and fineness modulus of fine aggregate were 2.78, 1662 kg/m^3, and 2.81, respectively. The specific gravity, bulk density, and fineness modulus of coarse aggregate were 2.60, 1585 kg/m^3, and 2.72, respectively. The primary chemical constituents of aggregates are silica (SiO_2), calcium carbonate ($CaCO_3$), iron oxide (Fe_2O_3), aluminum

oxide (Al_2O_3), and some other minerals. To achieve higher slump, better strength, and impermeability, the binder material, such as alccofine-1203, was utilized as SCM. The alccofine is a by-product of blast furnace slag. It is a micro-fine material with a low calcium silicate content and high reactivity due to its controlled granulation and unique particle size distribution. The specific gravity of alccofine was 2.71. The composites were mixed using water at pH range of 7.0 to 8.5. Furthermore, the high-range water-reducing chemical additive (MASTER GLENIUM 8233) was employed to enhance the workability of concrete without bleeding and segregation. Two different types of natural fibers, namely, banana and coir fibers with a density of 1.30 g/cm^3 and 1.10 g/cm^3, were selected for this investigation as shown in Figures 1 and 2. The fibers used in the study were collected from a locally available factory. Both of the fibers were obtained with a diameter of 1 mm and are chopped to a length of 40 mm. The chemical and physical properties of banana and coir fibers are shown in Table 3.

Table 1. Oxide composition of binder material.

Oxide (%)	CaO	Al_2O_3	Fe_2O_3	SiO_2	MgO	SO_3	K_2O	Na_2O	LOI
OPC	63.90	5.60	4.10	18.60	1.92	2.40	0.82	0.44	1.35
Alccofine	32.23	21.40	1.20	35.30	8.20	0.13	-	-	-

Table 2. Physical characteristics of binding substances.

Properties	Cement	Alccofine-1203
Specific gravity	3.14	2.71
Standard consistency	28.9%	-
Initial setting time	38 min	-
Final setting time	612 min	-



Figure 1. Chopped banana fiber.



Figure 2. Chopped coir fiber.

Table 3. Properties of fiber.

Description	Banana Fiber [1]	Coir Fiber [11]
Physical Properties		
Diameter (mm)	1	1
Length (mm)	40	40
Elastic Modulus (GPa)	9 to 16	6
Density (g/cm^3)	1.30	1.10
Chemical Properties		
Lignin (%)	18	40–45
Cellulose (%)	55	32–43
Pectin (%)	3.50	1.80
Hemicellulose (%)	15.90	-
Extractives (%)	8	-
Moisture (%)	-	8

2.2. Mixture Compositions

In accordance with IS 10262: 2019 [32], the concrete mixture was created for M70 grade, and the control mixture included 15% of alccofine for partial cement substitution. The water cement ratio for all mixtures was maintained at 0.29, and the mixed proportions of HSC are listed in Table 4. On the other hand, banana and coir fibers were added at 0.5%, 1%, 1.5%, and 2% by the concrete mixture volume. This study developed nine concrete mixtures, including one control mixture and others with natural fibers. To achieve workability, polycarboxylate ether-based superplasticizer was dosed at 1.5% by weight of cement. A concrete mixer was used to make concrete. First, the aggregates and fibers were mixed for 2 min to ensure uniform distribution, and the binder materials were added and uniformly blended for 1 min. Finally, water and superplasticizer were added and completely mixed for 2 min. The concrete mixture ID 'NFC BF 1' is derived as follows: NFC stands for natural fiber concrete, BF stands for fiber name, and the number indicates the fiber percentage added. Various tests were carried out to identify the characteristics of HSC, as shown in Table 5.

Table 4. Details of mixture proportions (kg/m^3).

Mixture ID	Cement	Alccofine	Sand	Stone Jelly	Water	SP	Fiber (%)	
							BF	CF
CC	435.36	76.83	692.76	1120.34	5.08	149	-	-
NFC BF0.5	435.36	76.83	692.76	1120.34	5.08	149	0.50	-
NFC BF1	435.36	76.83	692.76	1120.34	5.08	149	1.00	-
NFC BF1.5	435.36	76.83	692.76	1120.34	5.08	149	1.50	-
NFC BF2	435.36	76.83	692.76	1120.34	5.08	149	2.00	-
NFC CF0.5	435.36	76.83	692.76	1120.34	5.08	149	-	0.50
NFC CF1	435.36	76.83	692.76	1120.34	5.08	149	-	1.00
NFC CF1.5	435.36	76.83	692.76	1120.34	5.08	149	-	1.50
NFC CF2	435.36	76.83	692.76	1120.34	5.08	149	-	2.00

Table 5. Test conducted and number of specimens cast in this investigation.

Sl. No.	Name of the Experiment	Shape of the Specimen	Dimension of the Specimen (mm)	Number of Specimens *
1	Long-term compressive strength	Cube	100 × 100 × 100	9—mixture, 12 cubes for each mixture; Total: 108 cubes
2	Rapid chloride permeability	Cylinder	100 × 50	9—mixture, 12 cylinders for each mixture; Total: 108 cylinders
3	Sorptivity	Cylinder	100 × 50	9—mixture, 12 cylinders for each mixture; Total: 108 cylinders
4	Water absorption	Cylinder	100 × 100	9—mixture, 12 cylinders for each mixture; Total: 108 cylinders
5	Volume of permeable voids	Cylinder	100 × 100	9—mixture, 12 cylinders for each mixture; Total: 108 cylinders
6	Acid attack	Cube	100 × 100 × 100	9—mixture, 12 cubes for each mixture; Total: 108 cubes

* All specimens are water cured at ambient temperature and tested at 28, 56, 90, and 180 days.

2.3. Durability Properties

2.3.1. Long-Term Compressive Strength Test

The long-term compressive strength test of concrete was conducted at 28, 56, 90, and 180 days of water-cured specimen. The long-term compression strength test was conducted on 100 × 100 × 100 mm cubical specimens in accordance with IS 516: 2018 [33].

2.3.2. Rapid Chloride Permeability Test (RCPT)

The RCP test evaluated the concrete resistance to chloride ion penetration. This test monitors the amount of electrical current flowing through a concrete specimen of 50 mm in thickness and 100 mm in diameter during a period of 6 h in accordance with ASTM C1202-2019 [34]. Figures 3 and 4 illustrate the experimental setup and schematic view. From Figure 4, both the CC and NFC BF/NFC CF samples were subjected to a 60 V direct current applied across its ends during the test. In one sample, lead is placed in a sodium chloride (NaCl) solution, while in the other sample, it is immersed in a sodium hydroxide (NaOH) solution.



Figure 3. RCP test setup.

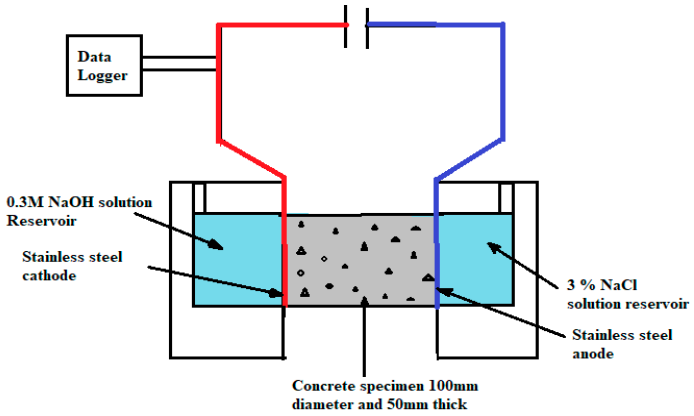


Figure 4. Schematic view of RCP test.

2.3.3. Sorptivity Test

To measure the amount of water in concrete pores through capillary action, the sorptivity test in accordance with ASTM C1585-2013 [35] was used. The specimens used in this experiment were 100 mm in diameter and 50 mm in thickness. Waterproofing material is placed on every surface of the sample, except for the one that will be in contact with water. Figure 5 illustrates the experimental setup.



Figure 5. Sorptivity test setup.

2.3.4. Water Absorption Test

The water absorption test was performed on cylindrical specimens with 100 mm in diameter and 100 mm in thickness. The cast cylinders were water cured for 28, 56, 90, and 180 days for this test. After water curing, the specimens were dried at 100 °C for 24 h in an oven. To determine the mass of sample (A), the specimens were allowed to cool in dry air after removal from the oven. Then, they were placed in water at 21 °C for at least 48 h. After immersion, the surface-dry mass (B) was determined. The percentage of water absorbed in hardened concrete was measured using the following calculation in accordance with ASTM C642-1997 [36]:

$$\text{Water absorption, \%} = [(B - A)/A] \times 100$$

2.3.5. Volume of Permeable Voids Test

The volume of permeable voids test was performed on cylindrical specimens with 100 mm in diameter and 100 mm in thickness. The cast cylinders were water cured for 28, 56, 90, and 180 days for this test. After water curing, the specimens were dried at 100 °C for 24 h in an oven. To determine the mass of sample (A), the specimens were allowed to cool in dry air after removal from the oven. Then, they were placed in water at 21 °C for

at least 48 h. After immersion, the surface-dry mass (B) was determined. Thereafter, the specimens were placed in a suitable container and boiled for 5 h using tap water. After cooling naturally for 14 h, the mass of specimen (C) was measured after wiping off the surface moisture. To determine the apparent mass of specimen in water, the specimens were suspended by a wire and the apparent weight (D) was measured. Finally, the volume of permeable voids was calculated in accordance with ASTM C642-1997 [36]:

$$\text{Volume of permeable pore voids, \%} = (C - A)/(C - D) \times 100$$

2.3.6. Acid Attack Test

A 100 mm cubical specimen was subjected to an acid attack investigation to evaluate the extent to which concrete resisted the acid regarding the preserved compressive strength. Concrete cubes were cast and water cured for 28 days for this investigation. The specimens were removed and left to dry for a day, and then the cube's initial weights were recorded. The concrete cubes were immersed for 28, 56, 90, and 180 days in diluted 5% sulphuric acid (H_2SO_4) solution with constant pH. The cubes were initially weighed, and then submerged in acid water for the whole period. The cubes' residual compressive strength is calculated after immersion in the acid water.

2.4. Microstructural Analysis

Microstructural characteristics of concrete blended with various proportions of both banana and coir fibers with alccofine were investigated after 180 days of water curing through scanning electron microscope (SEM), X-ray diffraction (XRD), and Fourier transform infrared (FTIR). The samples were collected from the inner core of the specimens, and then finely powdered. SEM analysis used a high resolution scanning electron microscope (HRSEM) with a 5 µm scale and 15,000× magnification. FTIR analysis focused on using a Bruker Alpha-T setup to envision the bonding effect of molecular category. Panalytical X'pert high score plus 2.2 software was utilized for XRD analysis to identify the crystalline phase of the material.

3. Results and Discussion

3.1. Long-Term Compressive Strength

Figures 6 and 7 display the results of the long-term compressive strength of HSC mixtures for various fiber combinations at varying curing ages. It should be noted that adding banana and coir fibers along with a specific amount of alccofine improves the compressive strength. The results for all the series show that the compressive strength, especially at 1% inclusion of banana fiber and 1% inclusion of coir fiber with alccofine, showed superior strength compared to the other mixtures for 28, 56, 90, and 180 days of water curing. This enhancement may be due to the developed physical and chemical properties of the fibers and binders. The long-term compressive strength was calculated to evaluate whether any decrease in strength or reversal of strength due to the addition of fibers, combined with exposure to water and other materials, was occurring. However, the compressive results showed that neither strength reversal nor strength reduction occurred in concrete mixtures containing or excluding fiber. Nevertheless, all concrete mixtures showed progressive strength gains up to 180 days. The NFC BF0.5, NFC BF1.5, and NFC CF0.5 mixtures moderately increased the compressive strength by 1.24%, 0.28%, and 0.21%, while NFC BF2, NFC CF1.5, and NFC CF2 mixtures reduced the compressive strength of concrete by 1.19%, 1.00%, and 1.30%, respectively compared to conventional HSC. According to the findings, at 1% fiber dosage, NFC BF1 and NFC CF1 mixtures showed a rise in compressive behavior at 1.51% and 1%, respectively, when correlated with source mixtures of HSC during a curing period of 180 days. Comparatively, NFC BF had a better strengthening effect than NFC CF. The strength augmentation occurred to the fiber and aggregate interlink system's influence, which prohibited and slowed down the great inception of micro-fissures. Moreover, alccofine fills the artery spaces in the matrix,

enhancing the strength performance of the matrix. Previous studies have noted a similar increase in compressive strength when fibers are incorporated [37].

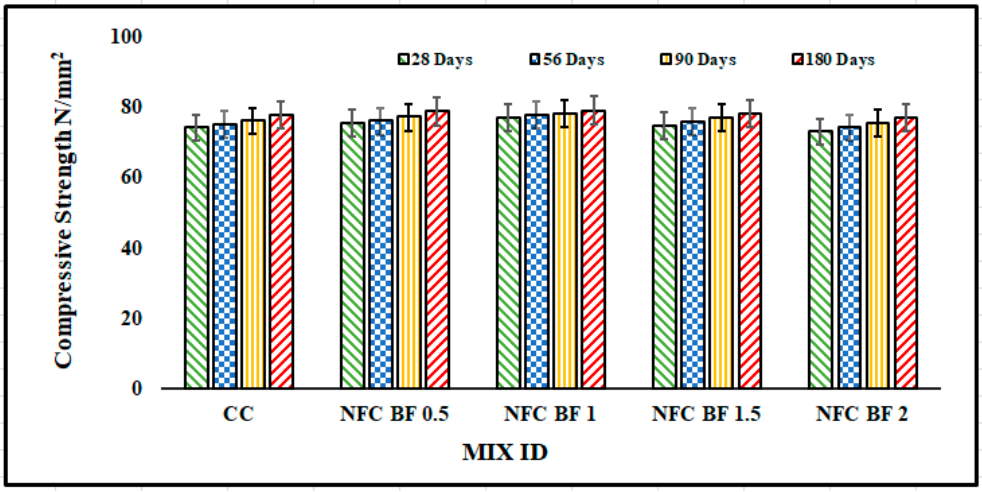


Figure 6. Compressive strength test outcomes of banana fiber concrete.

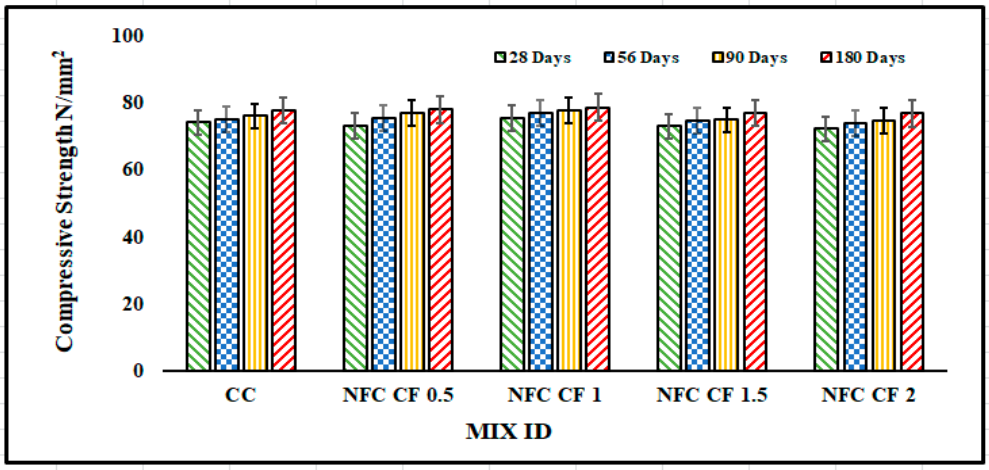


Figure 7. Compressive strength test outcomes of coir fiber concrete.

3.2. Water Absorption Test

A water absorption test was performed to estimate the porosity of concrete based on its ability to absorb water. The results of water absorption of all the mixtures, including one control mixture and the other containing natural fibers, are shown in Figures 8 and 9. From the figure, it is observed that the water absorption of BF-induced HSC at 1% dosage in the presence of alccofine reduced by 27.27%, while CF at 1% is reduced by 24.67%, compared to the control mixture after 180 days of curing. However, a slight increment is observed in the case of 1.5% and 2% in both BF- and CF-induced HSC. Therefore, BF absorbs less water when compared to CF due to the curling nature of BF fibers in concrete mixtures. In the case of CF, due to its stiff nature, they create voids and increase the water absorption tendency when compared with BF. However, the BF and CF blended with alccofine in concrete absorb less water since they are less brittle, shrink, and micro-crack susceptible when compared with other natural fibers [20].

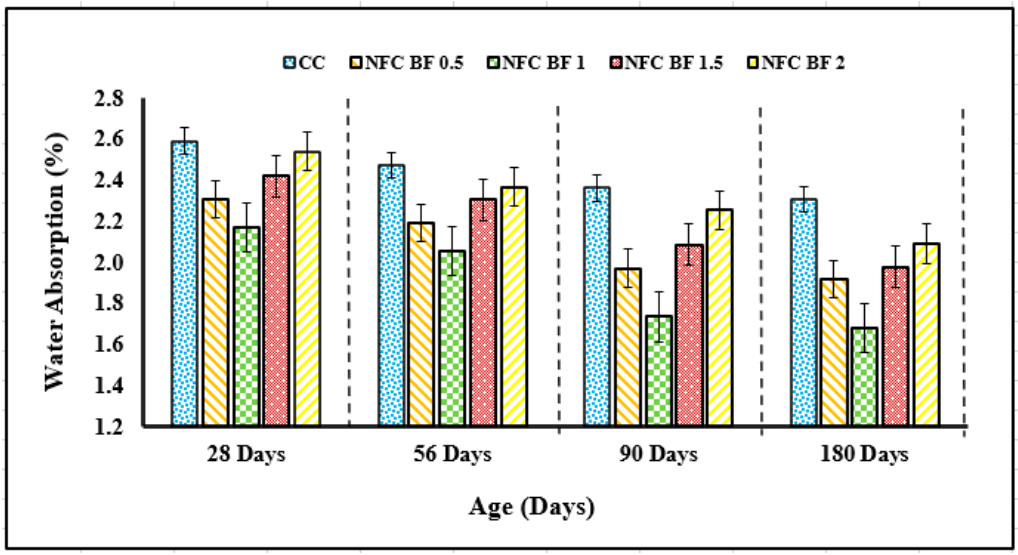


Figure 8. Water absorption test outcomes of banana fiber concrete.

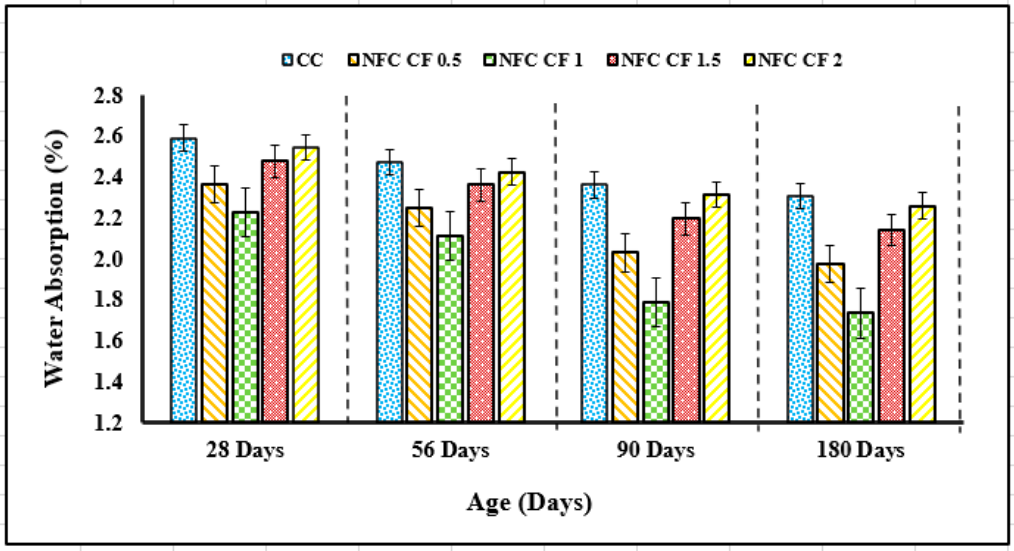


Figure 9. Water absorption test outcomes of coir fiber concrete.

3.3. Rapid Chloride Permeability Test

The RCPT outcomes of HSC mixtures for various percentages of banana and coir fibers (0.5%, 1%, 1.5%, and 2%) at 28, 56, 90, and 180 days of curing periods are displayed in Figures 10 and 11. A significant increase in chloride resistance is observed when banana and coir fibers are included compared to the control mixture. For all the mixture sequences, the obtained outcomes represent that the resistance to chloride permeability, particularly at the 1% addition of banana and coir fibers with alccofine showed higher levels than 0.5%, 1.5%, and 2%. The test outcomes showed that for a 1% dosage of natural fiber with alccofine, both NFC BF1 and NFC F1 mixtures showed a decrease in chloride permeability of 32.79% and 28.85% compared with conventional compounds, respectively, for a curing period of 180 days. The improved resistance to chloride permeability is attributed to the reduction in capillary porosity and inherent voids in concrete produced with banana and coir fibers and alccofine. Despite this, using banana and coir fibers in concrete above 1% resulted in an increase in entrapped air and the development of porosity. Similarly, Roja A. Nambiar and M.K. Haridharan [25] reported that concrete with fiber was more resistant

to chloride permeability. According to this study, fibers help in improving the concrete mixture packing density.

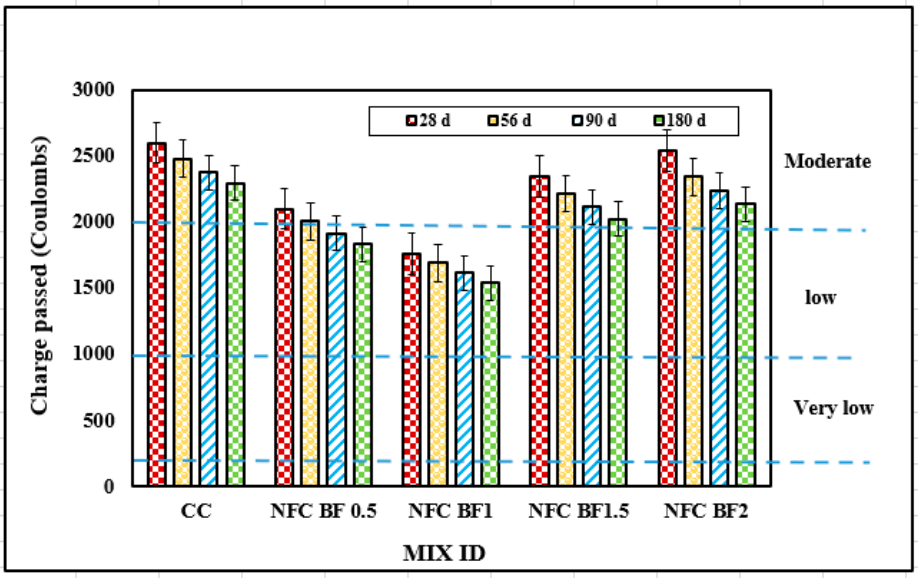


Figure 10. RCP test outcomes of banana fiber concrete.

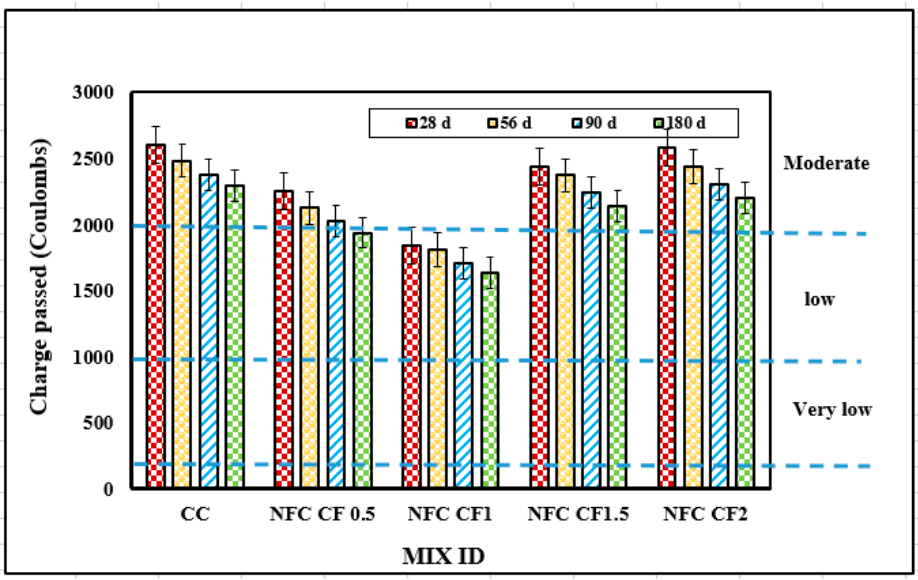


Figure 11. RCP test outcomes of coir fiber concrete.

3.4. Sorptivity Test

The sorptivity test results of concrete mixtures after 28, 56, 90 and 180 days are shown in Figures 12 and 13. Among all combinations, it was observed that the control mixture exhibited the highest sorptivity coefficient for concrete. However, relative to the control mixture, the concrete with banana and coir fibers and a fixed dosage of alccofine had a lower sorptivity coefficient. Both NFC BF1 and NFC CF1 mixtures had the lowest sorptivity coefficient, which was approximately 21.95% and 15.74% lower than the control mixture for a curing period of 180 days. Adding fiber to concrete decreases the concrete's capillary porosity and pores, resulting in reduced sorptivity. In another study, the sorptivity of concrete made with fiber decreased similarly [38]. It has been reported by Jayeshkumar Pitroda and F S Umrigar [38] that the integration of fibers decreased the sorptivity up to a specific volume proportion, then after this threshold, the sorptivity coefficient increased again.

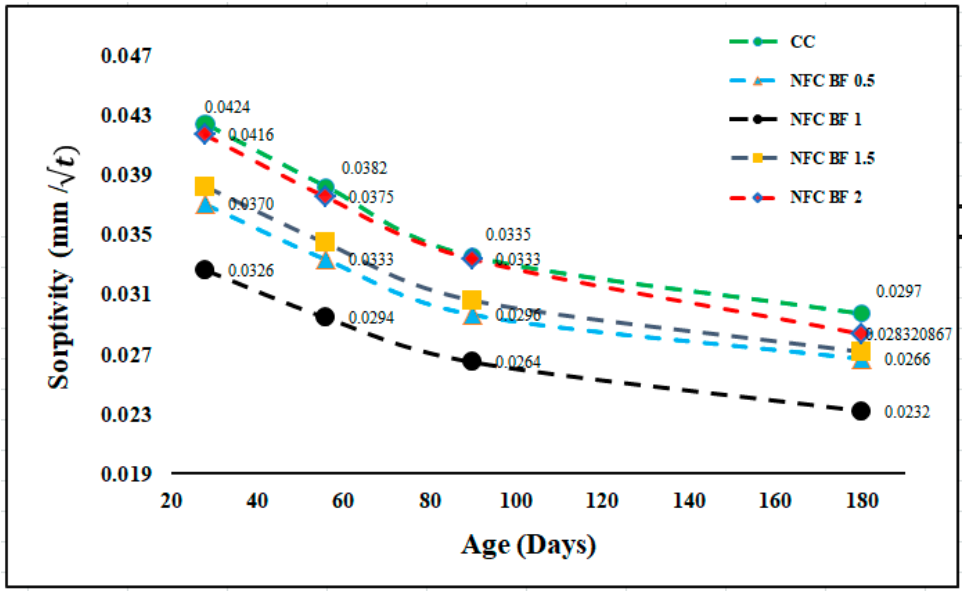


Figure 12. Sorptivity test outcomes of banana fiber concrete.

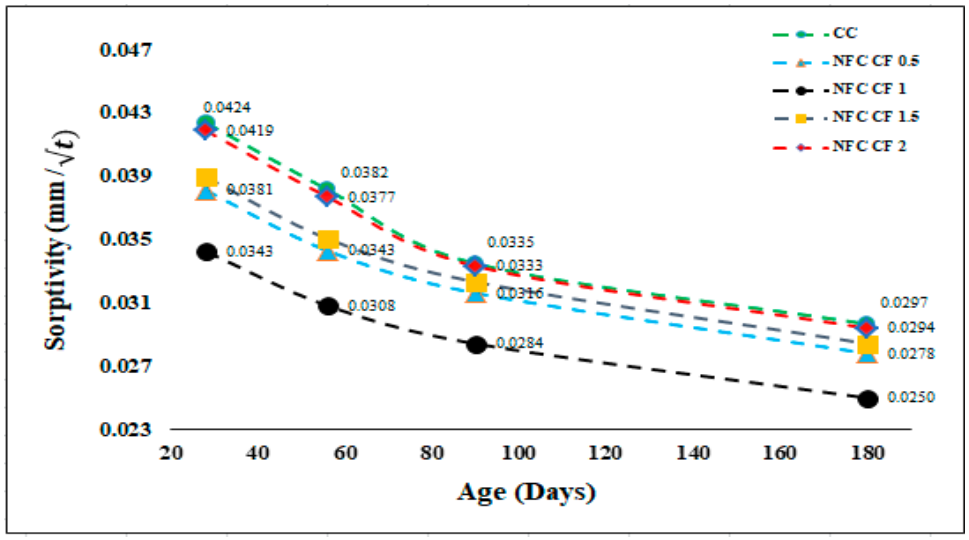


Figure 13. Sorptivity test outcomes of coir fiber concrete.

3.5. Volume of Permeable Voids Test

The volume of permeable voids test results of HSC mixtures for various percentages of banana and coir fibers (0.5%, 1%, 1.5%, and 2%) at 28, 56, 90, and 180 days of continual water curing are displayed in Figures 14 and 15. Among all combinations, the control mixture's volume of permeable voids for concrete was found to be the highest. However, relative to the control mixture, the concrete with 1% dosage of banana and coir fibers with a fixed amount of alccofine had a lower volume of permeable void. Based on the graphs, it can be concluded that the volume of permeable voids of BF at 1% dosage in the presence of alccofine-induced concrete decreased by 24.67% and CF at 1% dosage with alccofine-induced concrete reduced by 18.95%, compared to the control mixture after 180 days of curing. The denser structure with fiber-based particles is responsible for the reduced volume of permeable voids. Nitendra Palankar et al. [26] reported that incorporating fibers up to a specific volume proportion reduced the volume of permeable voids, and then after this level, the volume of permeable voids increased again.

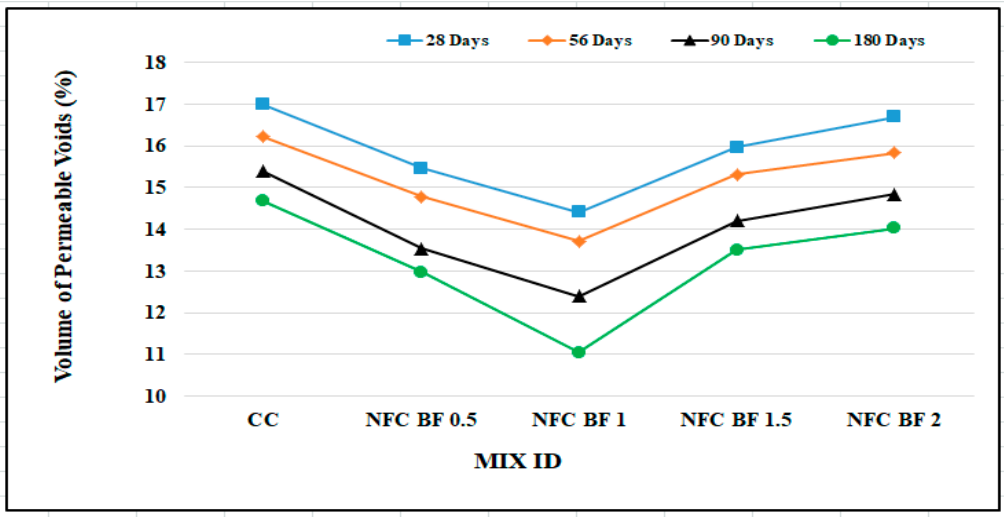


Figure 14. Volume of permeable voids test outcomes of banana fiber concrete.

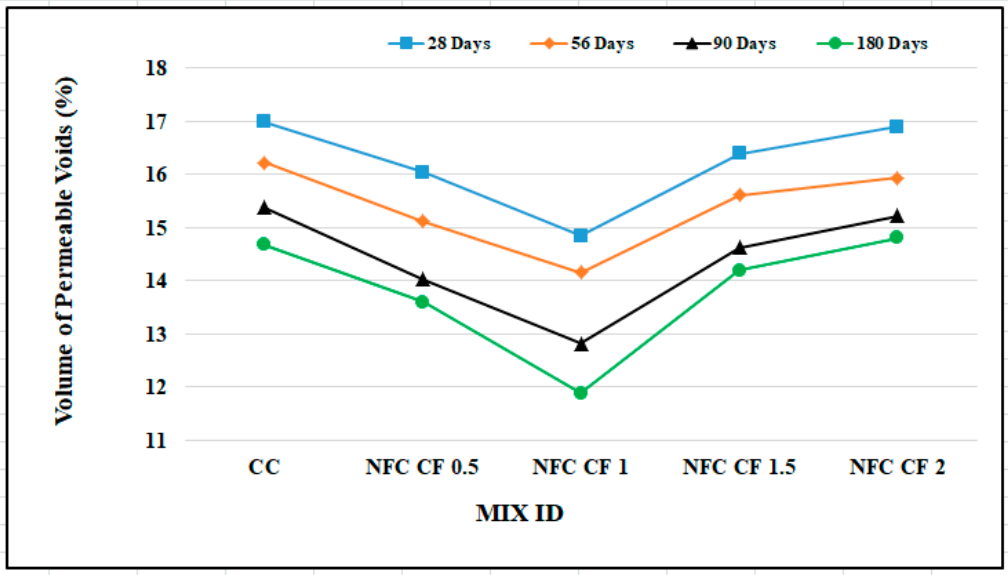


Figure 15. Volume of permeable voids test outcomes of coir fiber concrete.

3.6. Acid Attack Test

The compressive strength of various mixtures over time relative to HSC is displayed in Figures 16 and 17. As seen in Figures 16 and 17, all of the concrete mixtures gradually lose compressive strength over time after immersion in sulphuric acid solution. Compared to CC, NFC BF0.5, NFC BF1.5, NFC BF2, NFC CF0.5, NFC CF1.5, and NFC CF2, the NFC BF1 and NFC CF1 mixtures displayed superior resistance to acid attack. The characteristics and structures of the binders may show that the HSC mixtures blend with natural fiber up to 1% dosage, and alccofine illustrated excellent resistance to sulphuric acid than CC. Portlandite ($Ca(OH)_2$) and calcium silicate hydrate (CSH), which are susceptible to chemical deterioration, are the primary reaction products generated in OPC. OPC paste comprises $Ca(OH)_2$, calcium sulphoaluminates, and CSH on complete hydration. The calcium sulphoaluminates in OPC disintegrate at a pH below 11, whereas portlandite ($Ca(OH)_2$) prefers to disintegrate at a pH below 12. The CSH structure releases Ca^{2+} ions when the pH drops after exposure to a sulphuric acid environment [26]. Nevertheless, when the pH drops below 9, CSH loses its stability and releases most of the lime, leaving only a layer of silica and aluminosilicate gel that shields the uncorroded paste from further corrosion. The leaching of calcium is further controlled by the propagation of acids across

this layer. A highly porous corroded layer is left behind in cement under the impact of an acid environment due to the dissolving of hydrated products, such as portlandite and calcium sulphoaluminates, and the consequent decalcification of CSH formation, which lowers the compressive strength. As seen in Figure 15, the NFC BF1 showed a strength reduction in 41.24% relative to the NFC BF0.5, NFC BF1.5, and NFC BF2, which after spending 180 days of submersion in sulphuric acid solution, showed strength losses of 48.30%, 50.07%, and 52.87%, respectively. The NFC CF 0.5, NFC CF1, NFC CF1.5, and NFC CF2 mixtures all exhibit a similar decline in compressive strength with the addition of coir fiber. The deterioration of cement paste and aggregates caused by calcium dripping out of the aggregates may be responsible for the loss of strength.

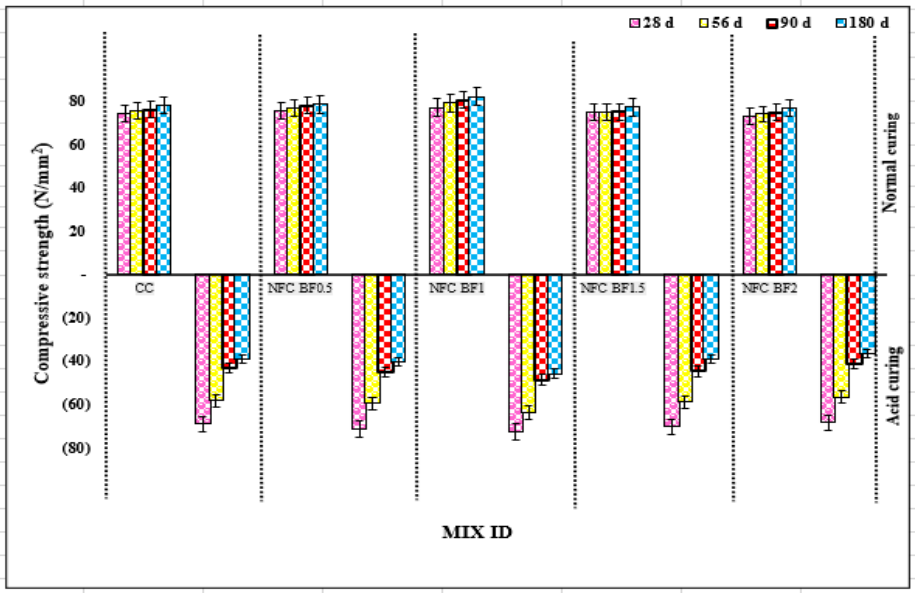


Figure 16. Compressive strength of acid attack test outcomes of banana fiber concrete.

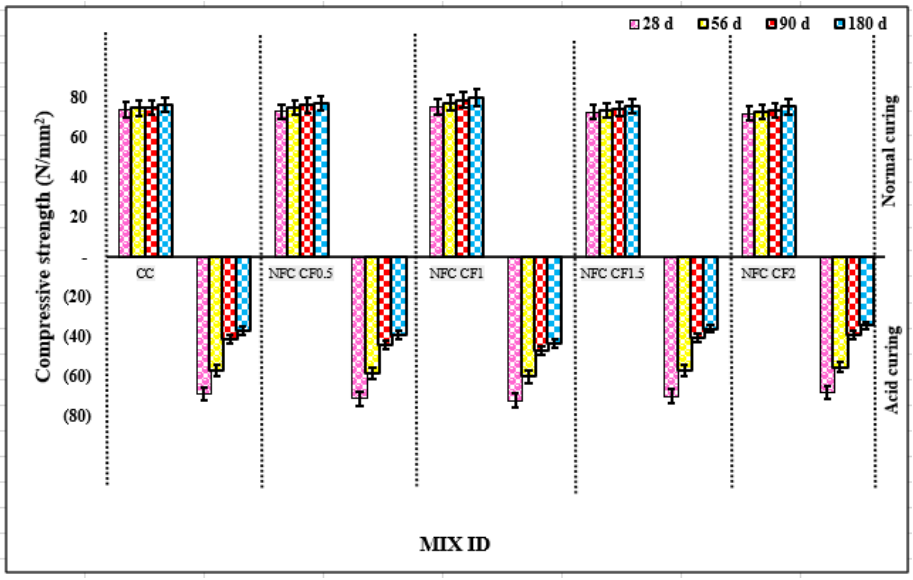


Figure 17. Compressive strength of acid attack test outcomes of coir fiber concrete.

3.7. SEM Analysis

SEM was used to study the microstructure of HSC concrete with various combinations of banana and coir fibers. The images of SEM of the control mixture and other mixtures after 180 days of curing are depicted in Figures 18–26, respectively, at a magnification of 15 kV, 15,000×. The SEM image of all mixtures revealed the distribution and formation of hydration products of hydrated cement paste concrete. The control concrete image of SEM showed that the surfaces were laminated with numerous voids and layers of disoriented hydrates, which may have weakened the concrete. In contrast, the SEM image of the NFC BF1 mixture indicated vast quantities of white crystals with tiny granular crystals on the surface, which elevated the strength of the concrete [39]. Alccofine added to concrete engendered more C-S-H gel, filling the gaps between voids and improving the mechanical properties. According to Figure 23, the highest strength was attained by incorporating a 1% dosage of banana fiber and alccofine, which is primarily attributed to forming a substantial amount of C-S-H gel. According to the SEM images, C-S-H gel production results in excellent cementitious bonding and the fibrous surfaces of banana and coir fibers created a robust interfacial connection between the cement matrix and the fiber. This behavior improved the interfacial adhesion, which helps in explaining that the strength properties of HSC have significantly improved. The matrix's density is increased by including 1% banana fiber and 1% coir fiber. After a 1% increase in the amount of fibers, the loose interfacial was discovered, which could be the primary factor for the degradation of concrete specimens. Figure 27 shows the interface between the fiber and the concrete. From the SEM image, it is observed that the surface of the fibers has a rough texture with hydrated and non-hydrated cement compound. This shows the good bond between the fiber and cement matrix.

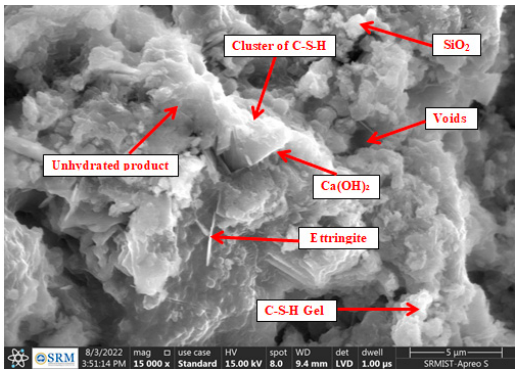


Figure 18. SEM image of CC.

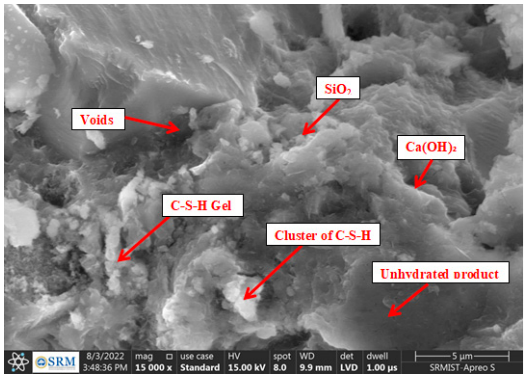


Figure 19. SEM image of NFC BF0.5.

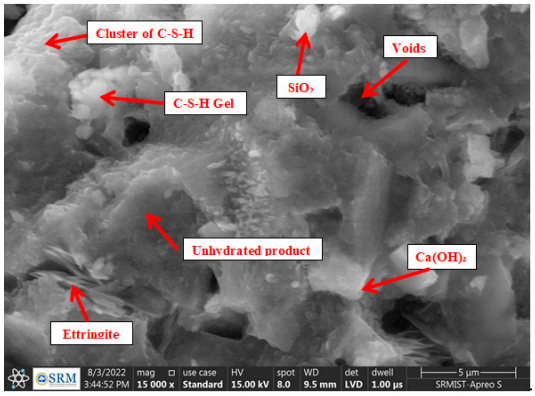


Figure 20. SEM image of NFC BF1.

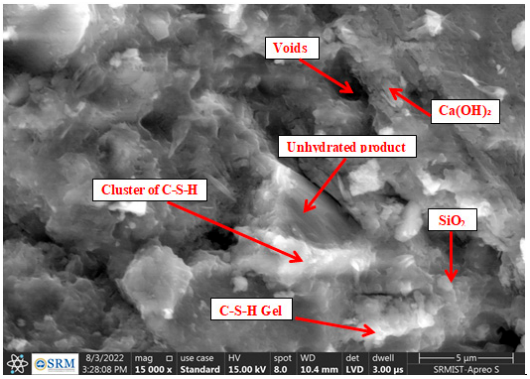


Figure 21. SEM image of NFC BF1.5.

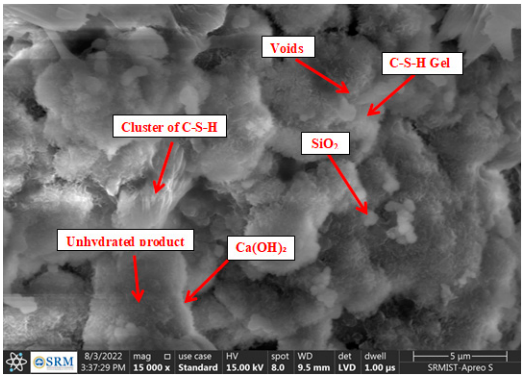


Figure 22. SEM image of NFC BF2.

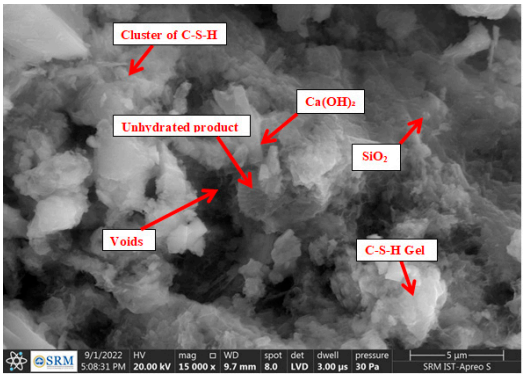


Figure 23. SEM image of NFC CF0.5.

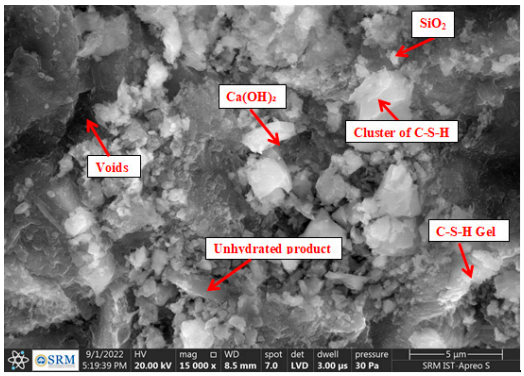


Figure 24. SEM image of NFC CF1.

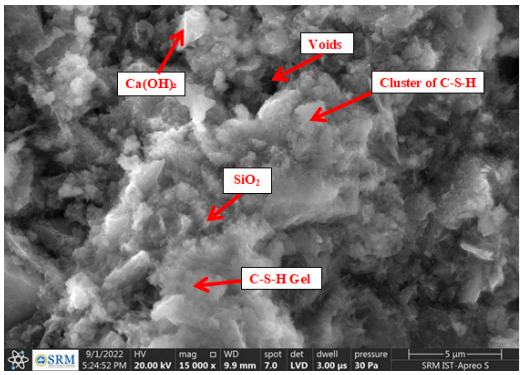


Figure 25. SEM image of NFC CF1.5.

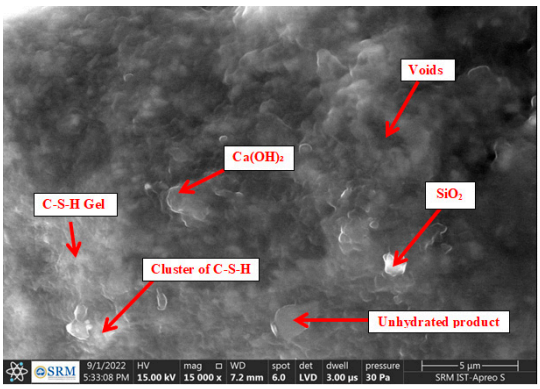


Figure 26. SEM image of NFC CF2.

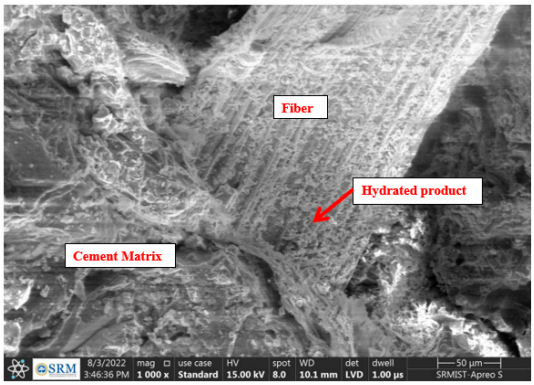


Figure 27. Interface between fiber and the concrete SEM image.

3.8. XRD Analysis

XRD analysis identified crystalline and semi-crystalline phases in the high-strength concrete with varying percentages of banana and coir fibers. XRD analysis was performed on samples obtained from each mixture. Figure 28 displays the XRD patterns of various HSC samples that were hydrated for 180 days. Quartz (SiO_2) and C-S-H were identified as prominent components by the typical peaks in the XRD pattern. In addition to calcite ($CaCO_3$), tricalcium silicate (C_3S), calcium hydroxide ($Ca(OH)_2$), and ettringite were detected in fiber concrete. These minerals are the predicted products of cement hydration. This pattern primarily denotes the presence of silica-based binder ingredients, such as cement, alccofine, and sand. The use of banana and coir fiber affects the proportions of portlandite, quartz, and other chemical components. In all mixtures, significant amounts of SiO_2 and C-S-H and trace amounts of ettringite were identified by the XRD pattern. The arrangement of fiber distribution inside the composite contributes to enhancing the mechanical properties. However, using fibers that are greater than 1.5% had a negative effect due to overdosing and settling.

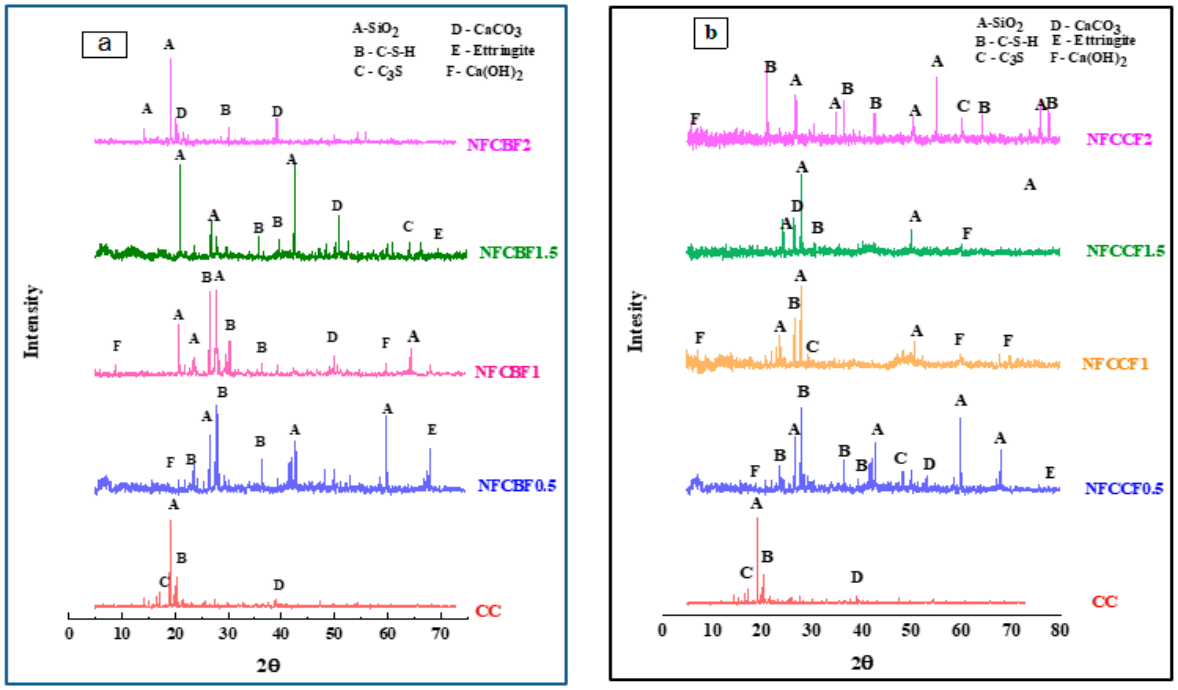


Figure 28. XRD analysis of fiber concrete. (**a**) Banana fiber, (**b**) coir fiber.

3.9. FTIR Analysis

Figures 29–37 depict the FTIR spectrum analysis of HSC mixtures with (0, 0.5%, 1%, 1.5%, and 2%) banana and coir fibers. FTIR spectrum identifies the presence of chemical interaction between materials in the HSC using the fusion spectrum. The existence of different chemical bonds in every sample at 180 days of water curing with a 400 cm^{-1} to 4000 cm^{-1} scanning range is exhibited in Figures 27–35. The presence of complex elements is indicated by peaks greater than five in the mixture. The firm intensity between 500 and 630 cm^{-1} is caused by the bending modes of SiO_6 that are present in all samples. The absorption intensity shows the O-H stretch bond at 3400 cm^{-1} to 4000 cm^{-1}, which was identified owing to the trembling of Ca $(OH)_2$ in NFC BF1 and NFC BF1. From the analysis, an unbending trembling of O-C-O at wavelengths between 900 cm^{-1} and 1100 cm^{-1} proves that the carbonation reaction is present. Ettringite is the cause of the neck bends seen at the top of 3600 cm^{-1}. Therefore, it is clear from the FTIR analysis that acuate bonds over 3500 cm^{-1} indicate the presence of oxygen-related bonding and thin bonds at 900 cm^{-1} indicate that SiO_4 is increased due to the addition of fiber and alccofine to the HSC mixtures.

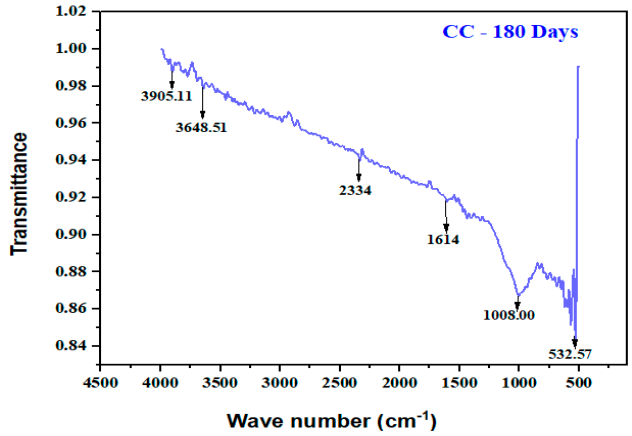


Figure 29. FTIR results of CC.

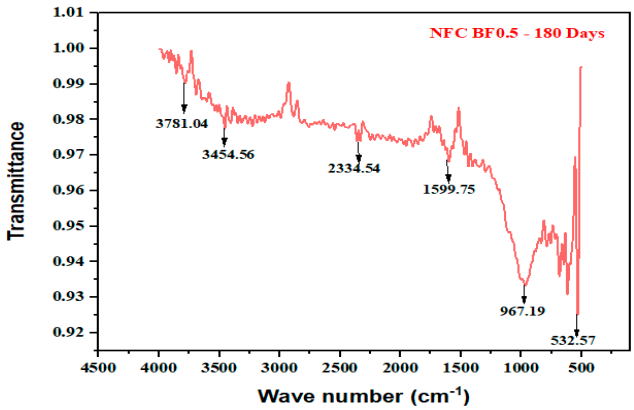


Figure 30. FTIR results of NFC BF0.5.

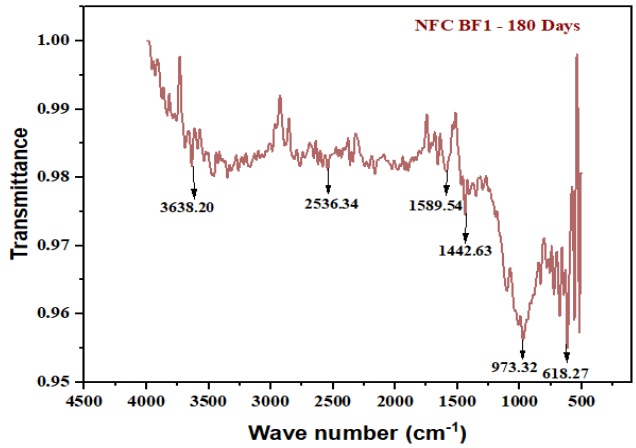


Figure 31. FTIR results of NFC BF1.

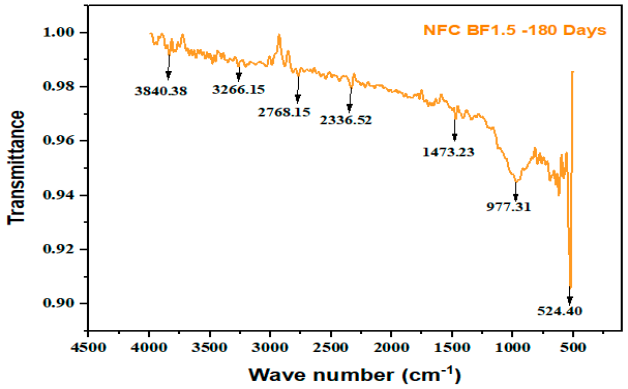


Figure 32. FTIR results of NFC BF1.5.

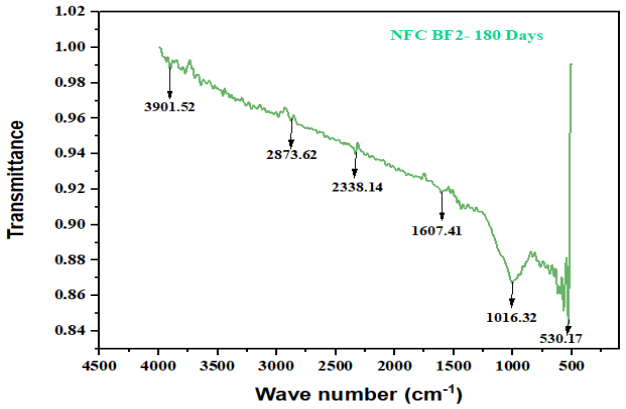


Figure 33. FTIR results of NFC BF2.

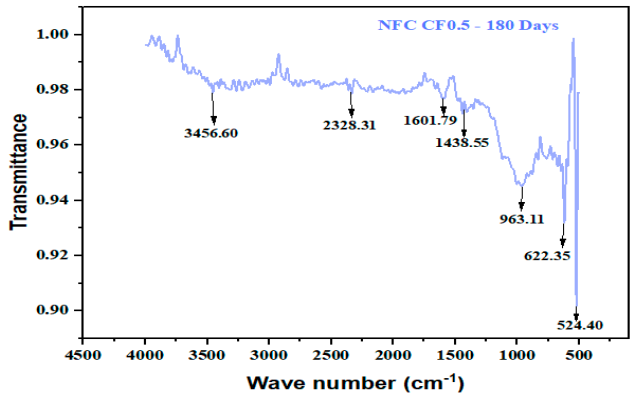


Figure 34. FTIR results of NFC CF0.5.

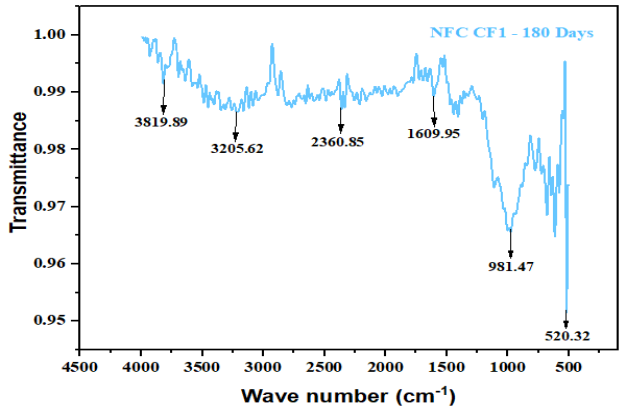


Figure 35. FTIR results of NFC CF1.

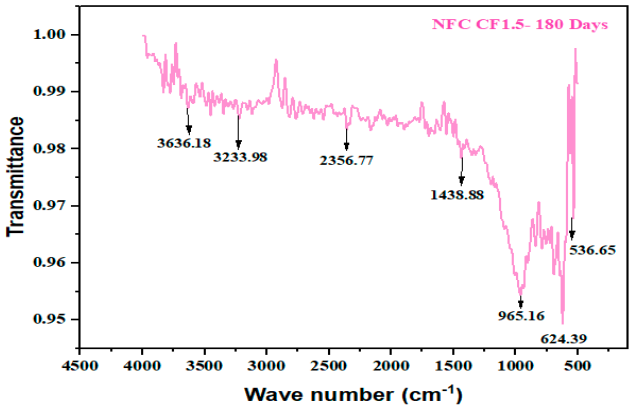


Figure 36. FTIR results of NFC CF1.5.

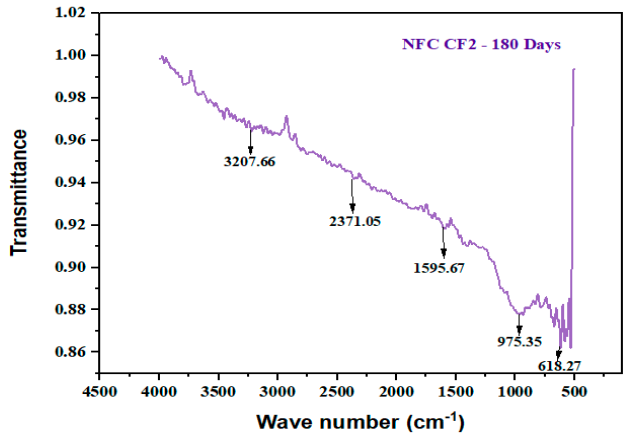


Figure 37. FTIR results of NFC CF2.

4. Conclusions

A comprehensive investigation is carried out in HSC with banana and coir fibers at different percentages. The durability properties, such as long-term compressive performance, rapid chloride penetration, water absorption, sorptivity, volume of permeable voids, and acid attack are evaluated. The microstructural study is also observed. The following findings were obtained:

- The addition of BF and CF in HSC significantly showed the strength enhancement at 1.51% and 1% when compared with the control mixture during its long-term compressive strength at 180 days of water curing.
- The integration of BF 1% and CF 1% combined with alccofine in HSC mixtures exhibited reduced coulomb passage, with 1540.50 and 1630.80 coulombs, respectively, after 180 days of water curing, when coulomb passage was compared to durability characteristics. Poor chloride ion permeability was discovered, and then coulomb's path started to increase.
- Compared to conventional concrete, the HSC created with alccofine containing 1% of BF and CF demonstrated superior resistance to acid environments, which may be linked to the characteristics and structures of binders.
- Alccofine and natural fibers, such as banana and coir fibers reduced the water absorption, sorptivity coefficient, and volume of permeable voids in concrete compared to the control mix. However, banana fiber had a more significant impact than coir fiber on the enhancement of the durability properties of concrete.
- At 1% fiber levels, BF and CF integration in HSC can produce tremendous durability improvements.

- The microstructural study visibly indicated the mechanical effectiveness of HSC mixtures with the intrusion of alccofine, BF, and CF. Conventional concrete produced voids and layers of disoriented hydrates than natural fiber concrete.
- The XRD analysis identified the crystalline phases present in the concrete incorporation of natural fibers and the FTIR analysis exhibited the carbonation process of natural fiber concrete.

Therefore, using natural fiber-based concrete is a viable option for construction purposes. Furthermore, this type of concrete is particularly suitable for constructing structural elements, such as beams and columns.

Author Contributions: Conceptualization and methodology, writing—original draft preparation, A.R.; validation, writing—review and editing, supervision and data curation, S.P.C.; formal analysis and supervision, P.T.R. All authors have read and agreed to the published version of the manuscript.

Funding: This research received no external funding.

Data Availability Statement: Not applicable.

Acknowledgments: I would like to thank SRM concrete technology laboratory, central instrumentation facility and NRC, Kattankulathur, for providing the microstructural characterization equipment, which the authors greatly acknowledge.

Conflicts of Interest: The authors declare no conflict of interest.

References

1. Dhawan, A.; Gupta, N.; Goyal, R.; Saxena, K. Evaluation of mechanical properties of concrete manufactured with fly ash, bagasse ash and banana fibre. *Mater. Today Proc.* **2021**, *44*, 17–22. [CrossRef]
2. Akid, A.S.M.; Hossain, S.; Munshi, I.U.; Elahi, M.A.; Sobuz, H.R.; Tam, V.W.; Islam, S. Assessing the influence of fly ash and polypropylene fiber on fresh, mechanical and durability properties of concrete. *J. King Saud Univ. Eng. Sci.* **2021**. [CrossRef]
3. Blazy, J.; Blazy, R. Polypropylene fiber reinforced concrete and its application in creating architectural forms of public spaces. *Case Stud. Constr. Mater.* **2021**, *14*, e00549. [CrossRef]
4. M, K.; Nachiar, S.S.; Sekar, A. Engineering Properties of Waste Badminton String Fiber. *Fibers* **2023**, *11*, 25. [CrossRef]
5. Mathew, B.A.; Sudha, C.; Kannan Rajkumar, P.R.; Ravichandran, P.T. Investigations on Tensile Properties of High Strength Steel Fibre Reinforced Concrete. *Indian J. Sci. Technol.* **2015**, *8*, 83–89. [CrossRef]
6. Ikumi, T.; Galeote, E.; Pujadas, P.; de la Fuente, A.; López-Carreño, R. Neural network-aided prediction of post-cracking tensile strength of fibre-reinforced concrete. *Comput. Struct.* **2021**, *256*, 106640. [CrossRef]
7. Long, W.; Wang, Y. Effect of pine needle fibre reinforcement on the mechanical properties of concrete. *Constr. Build. Mater.* **2021**, *278*, 122333. [CrossRef]
8. Wani, I.A.; Kumar, R.U.R. Experimental investigation on using sheep wool as fiber reinforcement in concrete giving increment in overall strength. *Mater. Today Proc.* **2021**, *45*, 4405–4409. [CrossRef]
9. Sabarish, K.V.; Paul, P.; Bhuvaneshwari; Jones, J. An experimental investigation on properties of sisal fiber used in the concrete. *Mater. Today Proc.* **2020**, *22*, 439–443. [CrossRef]
10. ACI Committee 544. IR-82, State-of-the-Art Report on Fiber Reinforced Shotcrete. *Concr. Int.* **1984**, *6*, 15–27.
11. Shah, I.; Li, J.; Yang, S.; Zhang, Y.; Anwar, A. Experimental Investigation on the Mechanical Properties of Natural Fiber Reinforced Concrete. *J. Renew. Mater.* **2022**, *10*, 1307–1320. [CrossRef]
12. Alomayri, T.; Yosri, A.M.; Ali, B.; Raza, S.S.; Yaqub, M.; Kurda, R.; Deifalla, A.F. The influence of coconut fibres and ground steel slag on strength and durability properties of recycled aggregate concrete: Sustainable design of fibre reinforced concrete. *J. Mater. Res. Technol.* **2023**, *24*, 10027–10039. [CrossRef]
13. Jirawattanasomkul, T.; Ueda, T.; Likitlersuang, S.; Zhang, D.; Hanwiboonwat, N.; Wuttiwannasak, N.; Horsangchai, K. Effect of natural fibre reinforced polymers on confined compressive strength of concrete. *Constr. Build. Mater.* **2019**, *223*, 156–164. [CrossRef]
14. Krishna, N.K.; Prasanth, M.; Gowtham, R.; Karthic, S.; Mini, K.M. Enhancement of properties of concrete using natural fibers. *Mater. Today Proc.* **2018**, *5*, 23816–23823. [CrossRef]
15. Kumar, P.; Roy, R. Study and experimental investigation of flow and flexural properties of natural fiber reinforced self compacting concrete. *Procedia Comput. Sci.* **2018**, *125*, 598–608. [CrossRef]
16. Syed, H.; Nerella, R.; Madduru, S.R.C. Role of coconut coir fiber in concrete. *Mater. Today Proc.* **2020**, *27*, 1104–1110. [CrossRef]
17. Asim, M.; Uddin, G.M.; Jamshaid, H.; Raza, A.; Tahir, Z.U.R.; Hussain, U.; Satti, A.N.; Hayat, N.; Arafat, S.M. Comparative experimental investigation of natural fibers reinforced light weight concrete as thermally efficient building materials. *J. Build. Eng.* **2020**, *31*, 101411. [CrossRef]

18. Chandar, S.P.; Gunasekaran, K.; NabeelBabu, V.P.; Potti, R. Experimental Investigation on the Mechanical Properties of Concrete Mixed with Banana Stem Fiber as Well as Hybrid Steel Fiber. *Rasayan J. Chem.* **2018**, *11*, 640–646. [CrossRef]
19. Zhang, D.; Tan, K.H.; Dasari, A.; Weng, Y. Effect of natural fibers on thermal spalling resistance of ultra-high performance concrete. *Cem. Concr. Compos.* **2020**, *109*, 103512. [CrossRef]
20. Ali, B.; Azab, M.; Ahmed, H.; Kurda, R.; El Ouni, M.H.; Elhag, A.B. Investigation of physical, strength, and ductility characteristics of concrete reinforced with banana (Musaceae) stem fiber. *J. Build. Eng.* **2022**, *61*, 105024. [CrossRef]
21. Ali, M.; Li, X.; Chouw, N. Experimental investigations on bond strength between coconut fibre and concrete. *Mater. Des.* **2013**, *44*, 596–605. [CrossRef]
22. Elbehiry, A.; Elnawawy, O.; Kassem, M.; Zaher, A.; Uddin, N.; Mostafa, M. Performance of concrete beams reinforced using banana fiber bars. *Case Stud. Constr. Mater.* **2020**, *13*, e00361. [CrossRef]
23. Swathi, V.; Asadi, S. Structural performance of hybrid fibres based concrete: Mechanical, durability and microstructural properties. *Sustain. Futures* **2022**, *4*, 100094. [CrossRef]
24. Madhavi, K.; Harshith, V.; Gangadhar, M.; Kumar, V.C.; Raghavendra, T. External strengthening of concrete with natural and synthetic fiber composites. *Mater. Today Proc.* **2020**, *38*, 2803–2809. [CrossRef]
25. Nambiar, R.A.; Haridharan, M. Mechanical and durability study of high performance concrete with addition of natural fiber (jute). *Mater. Today Proc.* **2019**, *46*, 4941–4947. [CrossRef]
26. Palankar, N.; Shankar, A.R.; Mithun, B.M. Durability studies on eco-friendly concrete mixes incorporating steel slag as coarse aggregates. *J. Clean. Prod.* **2016**, *129*, 437–448. [CrossRef]
27. Liu, C.J.; Hunag, X.C.; Wu, Y.-Y.; Deng, X.W.; Zheng, Z.L.; Yang, B. Studies on mechanical properties and durability of steel fiber reinforced concrete incorporating graphene oxide. *Cem. Concr. Compos.* **2022**, *130*, 104508. [CrossRef]
28. *IS 12269:2013*; Ordinary Portland Cement 53 Grade—Specification. Bureau of Indian Standards: New Delhi, India, 2013.
29. *IS: 4031 (Pat 4)—1988*; Methods of Physical Test for Hydraulic Cement, Determination of Consistency of Standard Cement Paste. Bureau of Indian Standards: New Delhi, India, 1988.
30. *IS: 4031 (Pat 5)—1988*; Methods of Physical Test for Hydraulic Cement, Determination of Initial and Final Setting Times. Bureau of Indian Standards: New Delhi, India, 1988.
31. *BIS 383—2016*; Coarse and Fine Aggregate from Natural Sources for Concrete. Bureau of Indian Standards: New Delhi, India, 2016.
32. *IS 10262*; Concrete Mix Proportioning—Guidelines. Bureau of Indian Standards: New Delhi, India, 2019.
33. *IS 516—2018*; Method of Tests for Strength of Concrete. Bureau of Indian Standards: New Delhi, India, 2018.
34. *ASTM C1202*; Standard Test Method for Electrical Indication of Concrete's Ability to Resist Chloride Ion Penetration. American Society for Testing and Materials: West Conshohocken, PA, USA, 2012.
35. *ASTM C1585-13*; Standard Test Method for Measurement of Rate of Absorption of Water by Hydraulic-Cement Concretes. ASTM International: West Conshohocken, PA, USA, 2018.
36. *ASTM C642*; Standard Test Method for Density, Absorption, and Voids in Hardened Concrete 1. American Society for Testing and Materials: West Conshohocken, PA, USA, 1997.
37. Sadrinejad, I.; Madandoust, R.; Ranjbar, M.M. The mechanical and durability properties of concrete containing hybrid synthetic fibers. *Constr. Build. Mater.* **2018**, *178*, 72–82. [CrossRef]
38. Pitroda, J.; Umrigar, F.S. Evaluation of Sorptivity and Water Absorption of Concrete with Partial Replacement of Cement by Thermal Industry Waste (Fly Ash). *ISO Certif. Int. J. Eng. Innov. Technol.* **2008**, *2*, 245–249.
39. Saran, A.S.A.; Magudeswaran, P. SEM Analysis on Sustainable High Performance Concrete. *Int. J. Innov. Res. Sci. Eng. Technol.* **2017**, *6*, 11.

Disclaimer/Publisher's Note: The statements, opinions and data contained in all publications are solely those of the individual author(s) and contributor(s) and not of MDPI and/or the editor(s). MDPI and/or the editor(s) disclaim responsibility for any injury to people or property resulting from any ideas, methods, instructions or products referred to in the content.